Chemical Engineering Journal 489 (2024) 151306

Contents lists available at ScienceDirect

Chemical Engineering Journal

journal homepage: www.elsevier.com/locate/cej

Application of thermodynamics to industrial grease production

Koottaparambil Lijesh [a], Roger A. Miller [b], Andrew Sanford [c], Jim Carroll [c], M.M. Khonsari [a,*]

[a] Department of Mechanical Engineering and Industrial Engineering, Louisiana State University, Baton Rouge, LA 70803, USA
[b] Consultant, 18342 Char A Banc, Baton Rouge, LA 70817, USA
[c] Schaeffer Manufacturing Co, Saint Louis, MO 63104, USA

ARTICLE INFO

Keywords:
Grease
Accumulative entropy generation (AEG)
Irreversible thermodynamics
Consistency

ABSTRACT

In-situ measurement technology is developed for the first time to monitor the complex reaction process involved in the reactors during the manufacturing of grease. The evolving rheological properties of the grease with raw material variations, environmental factors, and human errors demand precise control of process parameters. These complexities result in batch-to-batch inconsistencies, causing increased costs and lost manufacturing time. In-situ measurement of rheological properties during grease manufacturing can contribute to achieving a repeatable process by providing real-time feedback to the operator for timely adjustments as process deviations occur. In this paper, the rheological properties of grease are measured and displayed as the accumulated entropy generated (AEG), a parameter derived from the principles of irreversible thermodynamics. A process sensor unit (PSU) was developed to determine the AEG values of a 5000 kg grease kettle by measuring the real-time current and voltage of the kettle agitator and mill drives and the grease process temperature. The AEG value was determined for ten batches of NLGI grade 2 and five batches of NLGI grade 1.5 greases. The results confirmed a linear correlation between grease consistency and AEG values. A linear model is developed and programmed in the PSU to predict grease consistency.

1. Introduction

According to ASTM D288, grease is defined as a product consisting of a solid thickening agent (thickener) in a liquid lubricant (base oil) with additional ingredients (performance-enhancing additives) to provide specific properties [1]. In general, a grease consists of 65–95 wt% base oil, 5–35 wt% thickening agent, and 0– 15 wt% additives [2]. The ingredient types (base oils, thickeners, and additives) and their weight percentage—which are selected based on the application specifications— are formed, mixed, and homogenized in a grease kettle to manufacture grease. An appropriately formulated grease is expected to exhibit many desirable characteristics, such as delivering the correct viscosity, minimizing friction and wear on sliding surfaces [3], diminishing oxidation, and providing thermal stability for a wide range of operating conditions. These features make grease an ideal lubricant for many critical components used across various industries, including automotive, metalworking, power generation, robotics, and food and beverage processing [4,5].

Grease production requires conducting a reaction to create the thickener, agitating the mixture of base oils and additives, followed by homogenization of the product through a milling process to enhance the mechanical stability of the grease [6]. The process initiates with the in-situ development of the thickener, often referred to as ’soap,’ from the saponification reaction of fatty acids, followed by dehydration of the water developed as a by-product during the reaction. The soap is heated to the phase transition temperature, the product is cooled to soap crystallization, and the additives are added [7]. Ideally, at the end of the cooling process, a relatively compact microstructure of soap fibers is obtained with the desired rheological properties specified in terms of the grading scale set by the National Lubricating Grease Institute (NLGI) [8].

From a chemical point of view, the thickening of the grease product can be attributed to entanglement, van der Waals, capillary forces, polar attractive forces, etc. [9]. However, the fiber size and specific surface must be balanced to achieve mechanical stability [8]. Through homogenization, also referred to as the milling process, fibers undergo a transformation that results in their apparent shortening. This change is attributed to the attainment of higher specific surfaces of crystallites, where the intense mechanical action breaks down the fibers into finer particles [10]. This process enhances the inter-particle interactions and the attraction between the soap and oil, yielding higher mechanical

* Corresponding author.
E-mail address: khonsari@lsu.edu (M.M. Khonsari).

https://doi.org/10.1016/j.cej.2024.151306
Received 19 January 2024; Received in revised form 18 March 2024; Accepted 13 April 2024
Available online 16 April 2024

stability and improved rheological performance.

Fig. 1 shows the three primary reactions involved in the manufacturing of grease: (i) saponification reaction with heating until the transition point (maximum temperature), (ii) cooling of the product, and (iii) mixing of additives with homogenization while cooling of the product.

Aside from the process complexities described above, obtaining a repeatable grease consistency during every batch in single or multiple kettles is difficult due to the variations in the processing parameters such as texture (size and surface) of thickeners, the speed and duration of agitation and milling process, variations in the quality of the raw material and the ingredients addition time, heating, and cooling profiles [11–15]. Additional complications are due to the environmental conditions, particularly the ambient temperature. Instrument sensor drift, such as thermocouples or pressure transducers, can introduce variation into the process control scheme. As the batch nears completion, base oil is added or withheld to ensure the consistency meets the NLGI grade requirements. Consistency is measured by the penetration test (ASTM D 217). If batch consistency is too soft and does not meet NLGI grade specifications, the batch is downgraded, reworked, or sold as scrap. This results in extra handling costs and the loss of production efficiency.

The in-situ monitoring and process control technologies in industries provide insights and strategies for taking necessary corrective actions based on data measured [8,16–18]. One of the approaches to measure the in-situ rheological properties is determining the torque and/or power characteristic of a rotating motor and inserting it into the process stream during the manufacturing process. In laboratory scale experiments, Delgado *et al.* [8] and Franco *et al.* [17] demonstrated that measuring torque (and determining power) with processing time is useful for characterizing the evolution of the rheological properties of grease, the micro-structure of the fibers, and proposed models for determining the consistency index of the final grease product. Nevertheless, installing a torque sensor on an industrial-size grease kettle requires modification of the kettle, which can be costly. Further, the developed model does not consider all the necessary parameters, such as the temperature, rotational speed of the agitator, and weight of the ingredients required for characterizing the rheological property evolution of the grease.

The objective of the work is to develop a scientific methodology to quantify the evolution of grease rheological properties during their production in a kettle, by employing the theory of accumulative entropy generation (AEG)—a parameter derived in accordance with the principles of irreversible thermodynamics. The magnitude of AEG has been established to be constant for the conclusion of coating on a substrate material [19] and components under cyclic fatigue [20], under different constant and variable operating conditions. From these observations, the authors propose to validate the existence of a single value of AEG for the grease batch having the same consistency. The obtained AEG values will be correlated with grease consistency results via quality control (QC) checks.

The implementation of the approach will assist the industry in proactively predicting grease consistency, which can lead to timely operator intervention by adjusting the grease manufacturing process to achieve the desired consistency and reduce the waiting time for QC results. In the present work, the validation is carried out on an aluminum complex (AlC) grease manufactured on a 5000 kg industrial-size grease kettle. Values for AEG are determined by measuring the current and voltage of motor drives using current sensors, grease temperature using a thermocouple, and weight of the ingredients from load cells during reaction, agitation, and the homogenization process.

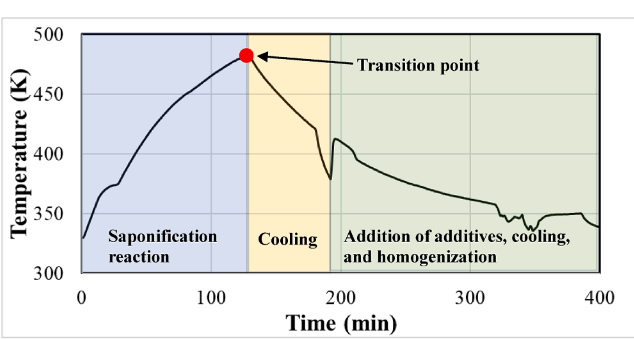

Fig. 1. Processes involved in grease production.

2. Methods

2.1. Manufacturing procedure for AlC grease

The general reaction process involved in developing the aluminum complex grease is shown in Eq. (1) [5]. The acid—stearic acid ($CH_3-(CH_2)_{16}-COOH$) and base—aluminum hydroxide ($Al(OH)_3$) are reacted to form soap (thickener)—aluminum tri-stearate ($[CH_3-(CH_2)_{16}-COO]_3Al$) with water ($H_2O$) as the by-product. The product of the neutralization process is mixed with a base oil and with necessary additives to obtain the final grease product.

$$CH_3-(CH_2)_{16}-COOH+Al(OH)_3\rightarrow[CH_3-(CH_2)_{16}-COO]_3Al+H_2O \tag{1}$$

The blending of the acids, bases, and base oil, followed by additives, is performed inside a grease kettle, which utilizes an agitator and a counter-rotating breaker bar driven by independent gear assemblies. The counter-rotation improves the internal circulation of the kettle contents and aids heat transfer as grease is continuously scrapped from the kettle wall and pushed towards the kettle shaft. The mixture can be heated or cooled in the kettle by circulating hot or cool oil through the kettle annulus via inlet and outlet ports shown in Fig. 2a. The setup is designed with valves to control the flow of the grease. The grease temperature is measured by a thermocouple inserted into the bulk grease nested in a thermowell.

The ingredients are added to the kettle by weight at intervals defined by the formulation chemistry. Kettle temperature is controlled to promote chemical reactions, formation of the thickener structure, and ingredient homogeneity. Typical trends for temperature, weight of the ingredients, and the rotating speed of the agitator during the different phases of AlC manufacturing are provided in Fig. 2b.

The manufacturing process involved in developing the AlC grease can be broadly consolidated into eight steps, as described below.

Step 1: The acids and base oil are added to the kettle. The mixture is blended at 60 rpm. While mixing, the kettle is heated to a temperature of 366 K (200 °F).

Step 2: At 366 K (200 °F), the base material is added to the mixture and agitated until the maximum temperature reaches 477 K (400 °F).

Step 3: The mixture is cooled to 422 K (300 °F).

Step 4: At 422 K (300 °F), the powders/flush oil are added to the mixture until the temperature reaches 394 K (250 °F) while mixing at 40 rpm. Further cooling continues until the temperature drops to 366 K (200 °F).

Step 5: The kettle contents are milled at 366 K (200 °F).

Step 6: At 366 K (200 °F), additives are added to the batch. Mixing continues at 20 rpm.

Step 7: The mixture is milled a second time. Mixing continues at 40 rpm.

Step 8: After the second milling phase is complete; everything is stopped, cooling continues, and a QC sample is taken.

These eight steps must be followed exactly to obtain a repeatable grease consistency in every batch. Any deviation in the steps will lead to deviation in the final grease consistency.

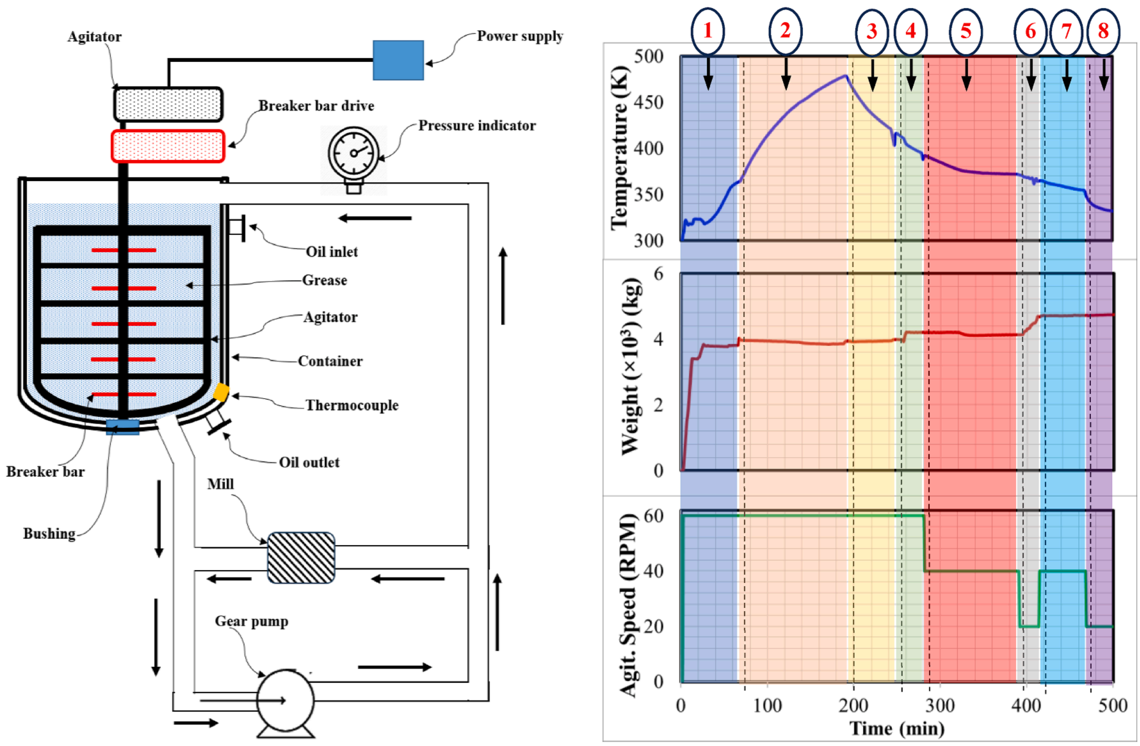

(a) (b)

Fig. 2. Schematic representation of the grease kettle and standard operating conditions and procedure. (a) grease kettle, (b) Temperature, weight, and agitator speed at different time intervals followed during grease manufacturing.

2.2. Mathematical modeling

A schematic representation of the grease manufacturing kettle is shown in Fig. 3. In the grease kettle, the outer kettle surface is stationary; the grease inside the kettle is sheared using a counter-rotating agitator at an angular speed of ω resulting in a shear rate of $\dot{\gamma}$. The system is considered a closed system, as there is no transfer of matter across the system. These reactions are characterized via the principles of irreversible thermodynamics [21–23]. According to the second law of thermodynamics, the change in entropy (dS) of an irreversible system monotonically increases until equilibrium or a stable state is reached [24]. Change in entropy is given by Eq. (2).

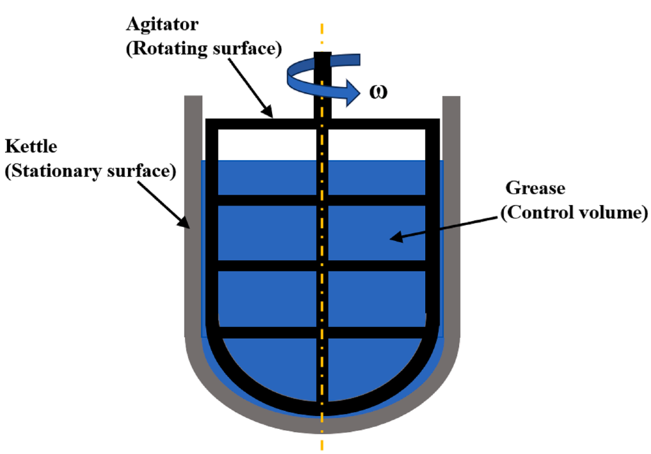

Fig. 3. Representation of the system considered for determining the entropy generation during the shearing of the grease inside a kettle.

$$dS = d_iS + d_eS \tag{2}$$

where d_iS is the entropy generated within the system, and d_eS is the entropy exchange with the environment [25–27]. In an irreversible system, d_iS is responsible for causing degradation and is always positive: $d_iS > 0$ [28]. Further, according to the second law of thermodynamics, dissipative systems generate entropy until the equilibrium state is reached and ceases to exist thereafter ($d_iS_{eq} = 0$) [23,25].

The entropy generated rate per unit volume during the shearing of the grease in the kettle is represented as $\dot{S}_g$, and is governed by the generalized thermodynamic forces, X, and generalized rates or flows, J terms, i.e., $\dot{S}_g = XJ$ [29–31]. Considering τ as the shear stress generated from shearing of the grease under a shear rate of $\dot{\gamma}$ at the grease temperature T, then, $\frac{\tau}{T}$ is the thermodynamic force X and $\dot{\gamma}$ is the thermodynamic flow J. The equation for $\dot{S}_g$ due to the shearing of grease is given by Eq. (3)

$$\dot{S}_g = \frac{\tau \bullet \dot{\gamma}}{T} \tag{3}$$

In Eq. (3), $\tau \bullet \dot{\gamma}$ can be replaced with the power required to shear the grease (P_{shear}) with unit volume (vol) i.e., $P/_{vol}$. Substituting $\tau \cdot \dot{\gamma} = P/_{vol}$ in Eq. (2) yields Eq. (4).

$$\dot{S}_g = \frac{P_{shear}}{T \bullet vol} \tag{4}$$

The power input required to shear the grease is determined by measuring the current and voltage of the kettle agitator drive. In a grease kettle, the total power (P) consumed during the shearing of the grease is the difference between the power required to rotate the agitator itself, P_o, and the power required to shear the grease, P_{shear}. Therefore, the power consumed during the shearing of the grease is determined by calculating the difference between the total power and the power consumed by the agitator drive when the kettle is empty (zero load). Thus, Eq. (4) can be written in the following form.

$$\dot{S}_g = \frac{P - P_o}{T \bullet vol} \quad (5)$$

As a general procedure, before starting production, the system is run without grease in the kettle, and the magnitude of P_o is recorded. The power consumed by the motor during the shearing operation is then determined by measuring the current and voltage. The current is measured by connecting a split core AC transducer sensor to one of the three-phase leads in the MCC (motor control center) and a constant voltage of 440 V is assumed. As mentioned earlier, the entropy generation is calculated on the agitator and mill motors. The values of instantaneous entropy generation for the agitator motor ($S_g(t)_{agi}$) and mill motor ($S_g(t)_{mil}$) are determined using Eqs. (6) and (7), respectively.

$$S_g(t)_{agi} = V\frac{\left(I(t)_{agi} - I_{0agi}\right)}{T(t) \times vol} \quad (6)$$

$$S_g(t)_{mil} = V\frac{\left(I(t)_{mil} - I_{0mil}\right)}{T(t) \times vol} \quad (7)$$

where V is the applied voltage, I_{0agi} and I_{0mil} are the no-load current of the agitator and mill motors, respectively, $I(t)_{agi}$ and $I(t)_{mil}$ are the instantaneous currents from the agitator and mill motors, respectively. It is hypothesized that batches adhering to the identical operating procedure outlined in Section 2.1, resulting in the same final grease consistency, will exhibit a constant value of accumulated entropy generation (AEG) up to the conclusion of the process. The AEG for the agitator and mill motor using Eqs. (6) and (7), respectively, are provided in Eq. (8) and (9), respectively.

$$\text{AEG}_{agi} = \int_0^t V\frac{\left(I(t)_{agi} - I_{0agi}\right)}{T(t) \times vol}dt = Constant \quad (8)$$

$$\text{AEG}_{mil} = \int_0^t V\frac{\left(I(t)_{mil} - I_{0mil}\right)}{T(t) \times vol}dt = Constant \quad (9)$$

2.3. Process sensor unit

To determine the AEG_{agi} and AEG_{mil} values during the grease manufacturing process, two current sensors are installed, one on the agitator and the other on the mill motors. The current sensors are connected to the wires of the agitator and mill motors in the control panel. The current measured with time from the agitator motor and mill motor are $I(t)_{agi}$ and $I(t)_{mil}$, respectively. Grease temperature is measured in real-time using a thermocouple. Ingredient weights are measured via load cells. All measured data is fed to the processing sensor unit (PSU). The PSU comprises a Raspberry Pi (a microprocessor) and a digital-to-analog converter. The PSU is programmed with Eqs. (8) and (9) to determine AEG_{agi} and AEG_{mil}. These accumulated entropies generated data are used for developing correlations with grease consistency. The real-time values of entropy generation, $S_g(t)_{agi}$, and $S_g(t)_{mil}$, are displayed in real-time to the operations engineer for making decisions on the process deviations. The engineer can adjust the process parameter to achieve the correct level of AEG, which will result in the desired batch consistency when processing is complete. All the results are displayed on a monitor. The following schematic connection diagram for the industrial-size grease kettle (5000 kg) for acquiring current from the agitator motor and the mill, load cell data, and the temperature from the thermocouple is shown in Fig. 4.

3. Results

3.1. Penetration test results (δ)

Field testing was conducted on a commercial-scale grease kettle available at Schaeffer Manufacturing Company, located in Saint Louis, Missouri. The consistency values for fifteen greases (comprising ten NLGI 2 and five 1.5 grade greases), obtained from the QC laboratory, are provided in Table 1. These consistency measurements are determined using the industrial standard penetration test (ASTM D217) [32]. From Table 1, the penetration values are observed to range between 275 and 306 dmm for Grade 2 grease, while 302 to 312 dmm, for Grade 1.5

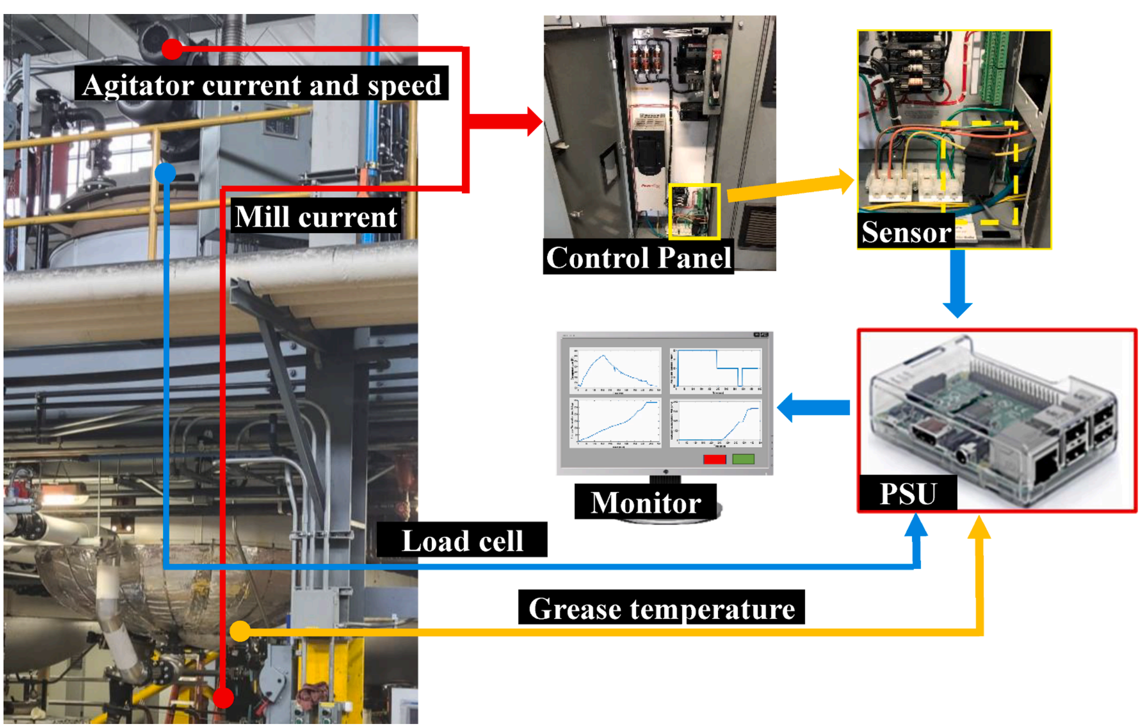

Fig. 4. Schematic presentation of current, weight, and temperature measurements from the grease kettle.

Table 1
Worked penetration, δ, reading from QC laboratory for NLGI 2 and 1.5-grade greases.

NLGI Grade	Grade 2										Grade 1.5				
Batch	1	2	3	4	5	6	7	8	9	10	11	12	13	14	15
δ (dmm)	275	275	285	302	282	287	295	295	306	283	302	302	302	305	312

grease. It is worth mentioning that for Batches 4 and 9, the penetration values are out of the specifications for Grade 2 (265–295 dmm) grease.

3.2. Correlation between AEG and δ

The AEG values for the considered fifteen batches are calculated from the real-time data of the weight of the ingredients, grease temperature, I_{agi}, and I_{mil} obtained from the PSU. As an example, Fig. 5a displays the real-time values of grease temperature and ingredient weights for Batch 1, while Fig. 5b presents the agitator and mill currents for the same batch.

Employing the real time data, the magnitude of $S_g(t)_{agi}$ and $S_g(t)_{mil}$ for fifteen batches is determined using Eqs. (6) and (7), respectively. The entropy generation data are normalized using the volume of the ingredients at a constant density of 900 kg/m^3. Further, no-load current for the agitator and mill motors, i.e., I_{0agi} and I_{0mil}, is required for calculating the $S_g(t)_{agi}$ and $S_g(t)_{mil}$, which is obtained by measuring the current from the current sensor, by running the motors at no load [33], i.e., without grease. The values of I_{0agi} and I_{0mil} were determined to be 13.5 and 5.0 A, respectively. Next, from $S_g(t)_{agi}$ and $S_g(t)_{mil}$, the AEG$_{agi}$, and AEG$_{mil}$ is determined until the completion of the second mill using Eqs. (8) and (9), respectively.

To develop a correlation between the AEG values with grease penetrations, the values of AEG$_{agi}$ and AEG$_{mil}$, are plotted against penetration (δ) for all fifteen batches in Fig. 6a and b, respectively. These figures illustrate a linear correlation between AEG$_{agi}$ and AEG$_{mil}$ with the grease consistency, with a coefficient of regression fit (R^2) of $\sim$ 0.93. The findings indicate that higher AEG values correspond to higher grease consistency (or lower grease penetration values). Therefore, we postulate that AEG determined from agitator and mill currents can be used to predict δ values for future batches.

From the linear fit data, the equations for predicting δ as a function of AEG$_{agi}$ and AEG$_{mil}$ are determined and provided in Eqs. (10) and (11). Both these equations are programmed into the PSU software to predict the δ of all future batches.

$$\delta = -0.45 \times \mathrm{AEG}_{agi} + 383 \quad (10)$$

$$\delta = -0.3 \times \mathrm{AEG}_{mil} + 376.6 \quad (11)$$

3.3. Control limits using the predictive models

The industry's foremost priority is to determine whether the final grease consistency meets the desired NLGI grade. For example, the specification of lower limit (LL) and upper limit (UL) of penetrations for NLGI 2 grade greases are 265 and 295 dmm, respectively, while for NLGI grade 1.5 grease, the LL and UL are 290 to 320 dmm, respectively. Our aim has been to develop a thermodynamic foundation for characterizing grease production to assist the operator in identifying whether the LL and UL of AEG values of the final grease consistency fall within this specified NLGI grade limit.

To determine the LL and UL of AEG$_{agi}$ and AEG$_{mil}$ corresponding to NLGI penetration ranges, the curve fit equation provided in Eqs. (10) and (11), respectively, are employed. Using Eqs. (10), the LL and UL for AEG$_{agi}$ corresponding to penetration ranges of 265 to 295 dmm for NLGI grade 2 grease is 261 to 195 kJ/K/m^3, respectively. Similarly, using Eqs. (11), the LL and UL for AEG$_{mil}$ for the same grade, grease is determined to be 362 to 265 J/K/m^3, respectively. Likewise, using Eq. (10) the LL and UL of AEG$_{agi}$ determined for Grade 1.5 grease with a penetration range of 290 to 320 dmm is 206 to 140 kJ/K/m^3, respectively, and for AEG$_{mil}$ is 282 to 184 J/K/m^3, respectively.

The AEG for NLGI grade 2 with the identified LL and UL of AEG$_{agi}$ and AEG$_{mil}$ are shown in Fig. 7a and b, respectively and for NLGI grade 1.5 greases are shown in Fig. 7c and d, respectively. Fig. 7a and b show that the measured AEG values for Batches 4 and 9 of Grade 2 grease are lower than the lower limit. Nonetheless, in the case of Grade 1.5, all the batches were within the identified upper and lower limits of AEG.

4. Discussions

4.1. Penetration

Examining the data in Table 1 reveals that despite following the same manufacturing procedures, variations in the penetration values are observed. To understand the reason for the variation in penetration values, ingredient weights, grease temperature, I_{agi}, and I_{mil}, of three Batches (1, 3, and 9) of NLGI 2 grease—having penetration values of 275, 285, and 306 dmm, respectively—are examined (see Fig. 8a-d).

From Fig. 8a-d, the following observations are made.

- From Fig. 8a, the weights of the ingredients until 200 min are nearly identical for all three batches; however, their weights differ by 207 kg between Batches 3 and 9. This reveals that the weights or

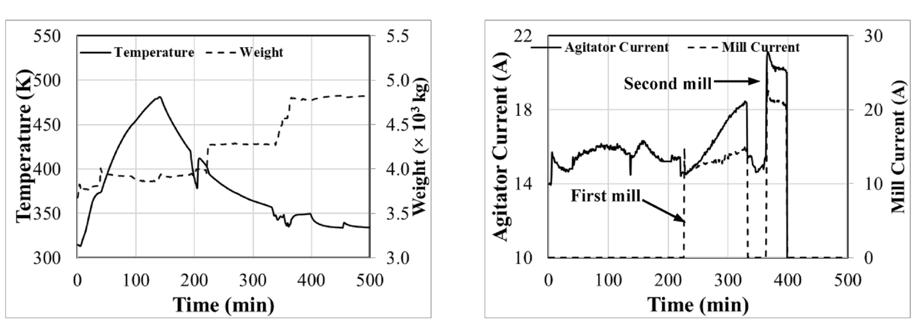

(a) (b)

Fig. 5. The measured weight of the accumulated ingredients, the temperature of the grease, and the currents from the agitator and mill motors with time for Batch 1. (a) Variation of the weight of the ingredients and temperature with time, (b) Variation of the agitator and mill motor current with time.

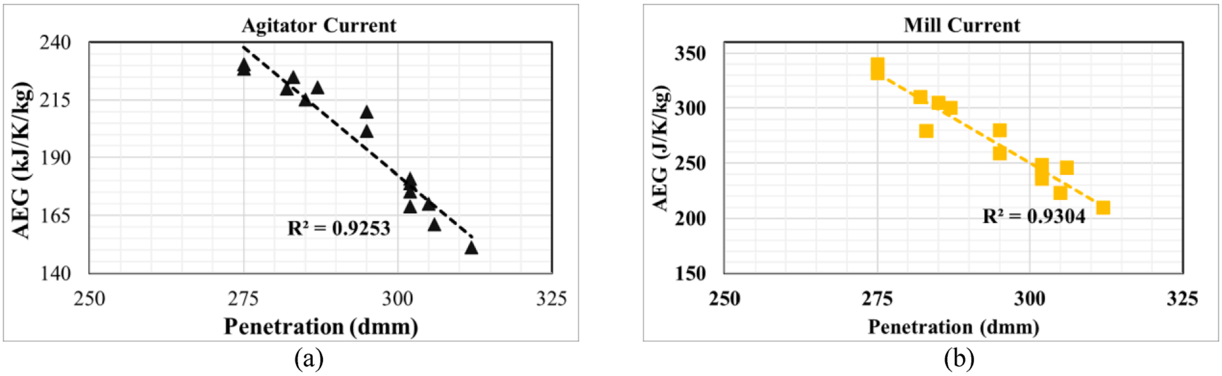

Fig. 6. AEG values identified from the agitator and mill current with the δ of the grease. (a) δ versus AEG value determined using the agitator current, (b) δ versus AEG value determined using the mill current.

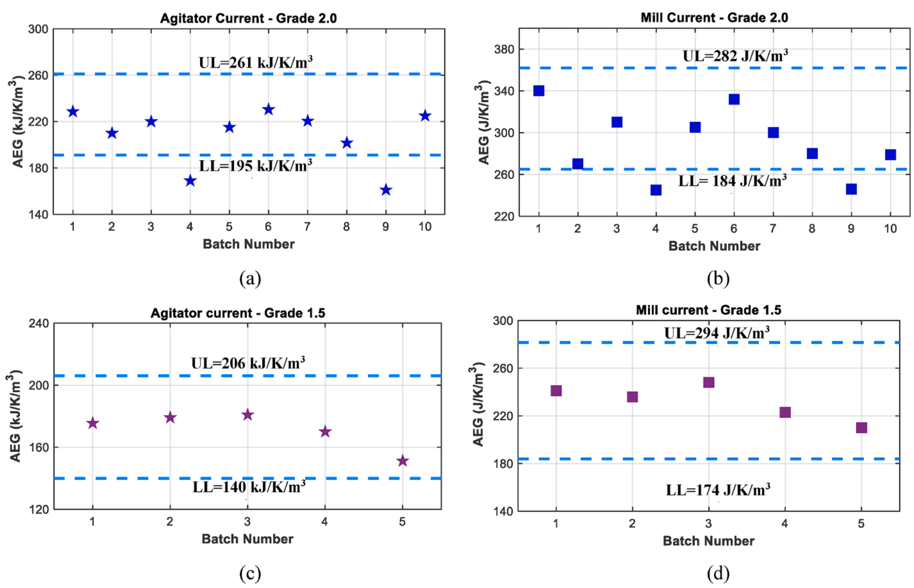

Fig. 7. Penetration for NLGI grade 2 and 1.5 greases with test numbers with upper and lower rages of entropy generation calculated from agitator and mill current. (a-b) Penetration readings for NLGI grade 2 grease with LL and UL calculated from agitator current and mill currents, respectively. (c-d) Penetration readings for NLGI grade 1.5 grease with LL and UL calculated from agitator current and mill currents, respectively.

quantities of powders/flush oil and additives added after 220 min were different, and we postulate that variation in the weight of raw materials could be one of the reasons for the deviation in the penetration values. Similar findings have been reported by several researchers [34–36], indicating that the weights of each raw materials added to the mixture have a considerable effect on the final consistency of the grease.

- From Fig. 8b, the maximum temperature is reached earlier for Batch 1, 142 min, followed by Batches 3 and 9, 158 and 163 min, respectively. Further, the duration of manufacturing from the beginning of the operation until the completion of the second milling process for Batches 1, 3, and 9 is 398, 417, and 435 min, respectively. These observations suggest varying reaction rates among different batches. McGuire [34] has pointed out that the final consistency of the grease product is dependent on the reaction rates, and to achieve repeatable consistency in every batch, the reaction rates need to be consistent.
- Referring to Fig. 8c and d, the total milling operation time for Batches 1, 3, and 9 is 171, 159, and 151 min, respectively. Coleman et al. [37] emphasized that, in manufacturing AlC grease, both the duration and temperature during the milling process are critical factors in attaining a consistent penetration value.

From the above discussion, it is concluded that grease manufacturing is very complex and prone to fluctuations during production, leading to variations in the final consistencies of the grease.

4.2. AEG

From Fig. 6a and b, it is evident that the proposed AEG values derived from the agitator and mill currents can effectively characterize the variation in penetration (δ) values across different batches and grades. To comprehend the reason behind the AEG value in characterizing the variation with δ, we proceeded to examine the AEG values calculated for Batches 1, 3, and 9. For this purpose, the values of AEG_{agi} and AEG_{mil} were determined using Eqs. (8) and (9), and the values are plotted in Fig. 9a and b, respectively. Referring to Fig. 9a, it is apparent that the values of AEG_{agi} remain consistent for all three batches until 250 min, after which a deviation occurs. Notably, from Fig. 8a, it is observed that the quantity of additives added to the mixture differed after 220 min, potentially explaining the deviation in the AEG value and final consistency.

Referring to Fig. 9a, the AEG values through the completion of the process based on the agitator's current (AEG_{agi}) for Batches 1, 3, and 9 are 219, 182.7, and 151 kJ/K/m^3, respectively. Similarly, using mill

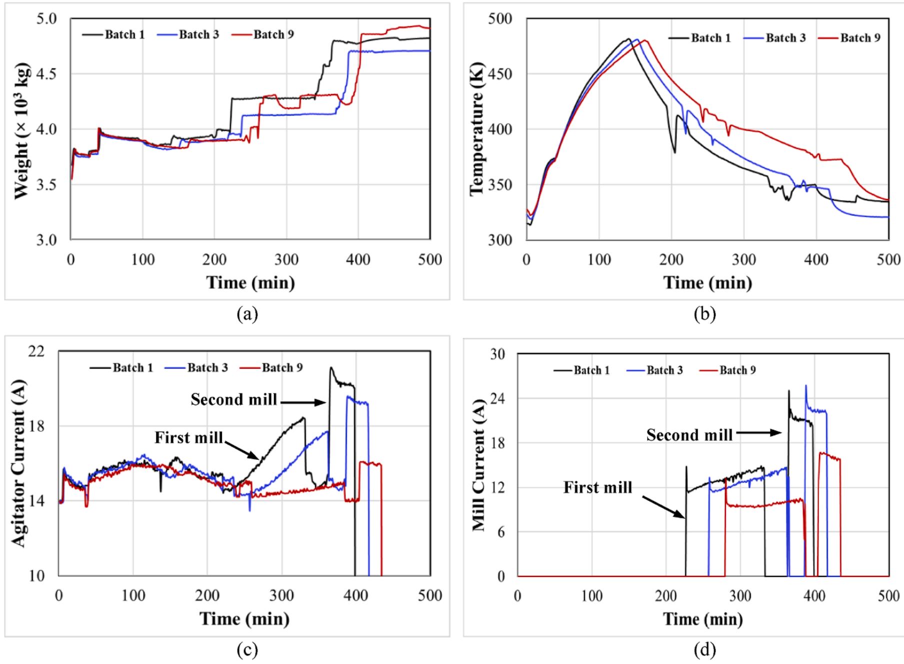

Fig. 8. The measured weight of the accumulated ingredients, the temperature of the grease, and the currents from the agitator and mill motors with time. (a) Variation of the weight of the ingredients with time, (b) Variation of the grease temperature with time, (c) Variation of the agitator motor current with time, (d) Variation of the mill motor current with time.

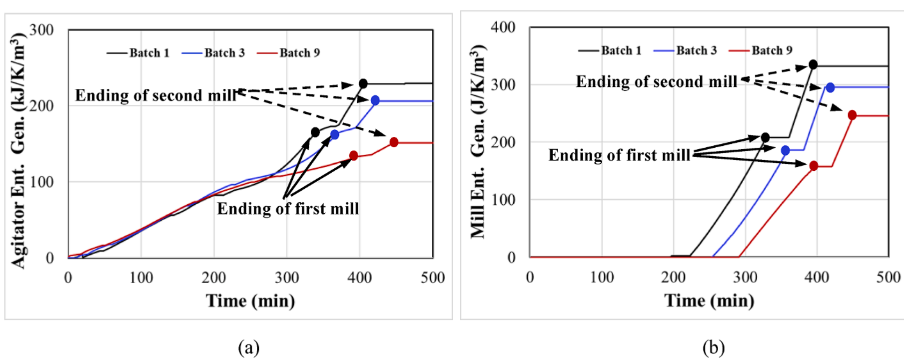

Fig. 9. The cumulative entropy generation calculated from the measured agitator and mill currents. (a) Agitator current, (b) Mill current.

current, the AEG values (AEG_{mil}) are determined to be 332, 295, and 246 J/K/m^3, respectively (see Fig. 9b). Comparing the values of δ (275, 285, and 306 dmm) of Batches 1, 3, and 9 with the maximum AEG_{agi} and AEG_{mil}, it becomes evident that penetration monotonically decreased with different AEG's through the completion of the process. In other words, the consistency of the grease monotonically increases with AEG's value. Such observation has been reported for components experiencing fatigue, where the material having higher life under fatigue will have higher entropy generation to failure [38,39]. For example, the entropy to failure for Al 6061-T6 and SS 304 materials were $\sim$ 4 and $\sim$ 60 MJm^{-3}K^{-1}, respectively. The values were roughly constant for

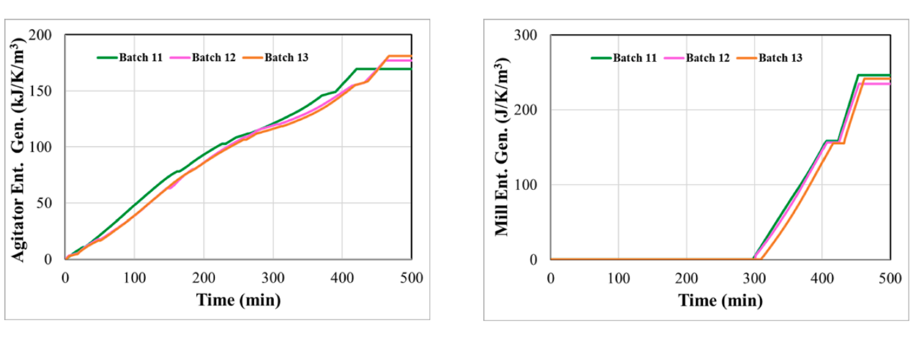

Fig. 10. The evolution of accumulative entropy generation calculated for the greases having 302 dmm penetration values using (a) Agitator current, (b) Mill current.

different specimen thicknesses, operating frequencies, and displacement amplitudes.

4.2.1. AEG for constant δ

Next, we tested the validity of Eqs. (8) and (9), i.e., the hypothesis that AEG values must be constant for grease batches having the same consistency and the manufacturing time in approximately same. We examined three Batches 11–13 of NLGI grade 1.5 greases, which had the same penetration of 302 dmm. The values of AEG_{agi} and AEG_{mil} determined using Eqs. (8) and (9) are plotted in Fig. 10a and b, respectively. The evolution of the entropy generation determined using the agitator current, AEG_{agi} for Batches 11–13 is observed to follow the same path for all three batches (see Fig. 10a) and the values of AEG_{agi} is identified to be 175.5, 179, and 181 kJ/K/m^3, respectively. Similarly, the AEG_{mil} determined from Fig. 10b for Batches 11–13 are 241, 236, and 248 J/K/m^3, respectively. Comparing the values AEG_{agi} and AEG_{mil} with the penetration values of Batches 11–13, it can be confirmed that for the batches having the same penetration value, the AEG values are approximately the same.

From the above discussion, it can be deduced that the batches having the same consistency will have the same AEG value at the conclusion of the process and conversely, batches having different consistency will have different AEG values.

4.3. Application of AEG

The proposed method of utilizing AEG facilitates early prediction of potential issues during grease manufacturing, assisting operational personnel in preemptively implementing corrective measures. The approach requires identifying a standard batch from the test batches, by examining the temperature behavior, the weights of the ingredients added, and the penetration values within the NLGI grade limits. The evolution curve of the AEG of the standard batch is programmed to the PSU and the real-time AEG value of the test batch is compared. When a process engineer or operator detects a deviation from the standard curve, pre-emptive actions can be taken. These actions include making process parameter adjustments or formulation ingredient additions or subtractions. For example, suppose the real-time entropy generation value is observed to have a higher magnitude than the standard value, indicating higher consistency. In that case, the engineer can add base oil to the product or alter the milling process to attain the right consistency.

For demonstration, we consider Batches 4 and 9, which were reported as the out-of-specification data (see Table 1). Examining the batches of Grade 2, Batch 3 is considered the standard batch, with a penetration value of 285 dmm. To comprehend the discrepancy between Batches 3 and 4, the evolution of AEG for Batches 3 and 4 is plotted in Fig. 11a. Fig. 11a shows that the deviation between the AEG values of Batches 3 and 4 is ~ 100 min. To understand the deviation, an investigation of the profiles of the weight of the ingredients, temperature, and rotational speed of the agitator was performed, and we observed the agitating speed for Batch 9 was different from the standard batch (Batch 3), from ~ 100 min. The overlay plot of agitator speed from Batches 3 and 9 is plotted in Fig. 11b. The change in the agitator speed affects the consistency index and the viscoelasticity of the grease [17]. The lower rotational speed of the agitator leads to altered heat transfer, consequently resulting in a different evolution of rheological properties. In this case, the operational person could correct the rotational speed of the agitator to achieve the right consistency.

To determine the cause of Batch 9 falling out of specification, an analysis is carried out by comparing the AEG values between Batch 3 (standard batch) and Batch 9. The AEG values of Batches 3 and 9 are plotted in Fig. 12a and from this figure the point of deviation is observed at ~ 180 min. As discussed earlier in Section 4.1, the reason for the deviation is identified to be due to different reaction rates. This was confirmed by referring to Fig. 12b, which shows that the time to reach the maximum temperature for Batch 9 (1 6 3) is more than the standard batch (1 5 8). Also the cooling rate of the mixture is observed to be lower for Batch 9. To achieve the correct final consistency, the operational personnel can adjust the cooling rate to match the cooling rate of the standard curve.

Batches 4 and 9, which have different desired consistency, will be subsequently re-worked and re-graded to meet a proper NLGI grade. Nevertheless, before releasing the batches to the market, it is assured that all quality control testing is passed.

5. Conclusions

In this work, we developed a procedure for applying the second law of thermodynamics to the grease manufacturing process to achieve the desired consistency confidently. The approach was field-tested in a grease manufacturing plant. The importance of this approach stems from the need for grease manufacturing, which is known to experience significant rheological variations during processing. More specifically, a batch process used to manufacture lubricating grease was used to model the relationship between generated entropy from thermal and mechanical sources and a specific measure of product rheology relating to product consistency. A process sensor unit was developed to collect analog data from the continuous calculation of entropy generation. The authors found the relationship between the kettle agitator-generated entropy and the shearing operations-generated entropy to have very strong linear relationships to the key consistency test. Using these reference data, the authors propose an ideal curve for typical batches that can be programmed into the sensor unit to provide real-time feedback to operator personnel. Additionally, the linear relationship between generated entropy and consistency can be used to model the upper and lower entropy control limits that correlate with consistency product specifications to provide feedback on batch control at critical points in manufacture. Importantly, the results of extensive testing reveal that accumulated generated entropy is relatively constant for batches meeting the product specifications.

CRediT authorship contribution statement

Koottaparambil Lijesh: . **Roger A. Miller:** Writing – review &

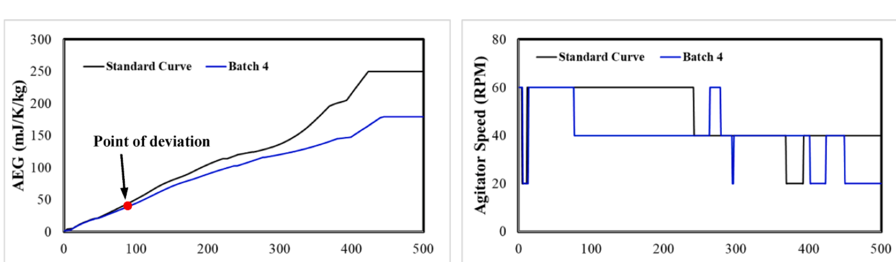

(a) (b)

Fig. 11. Comparison of Batch 4 with the standard batch (Batch 3) (a) Comparison of AEG value, (b) Comparison of agitator RPM.

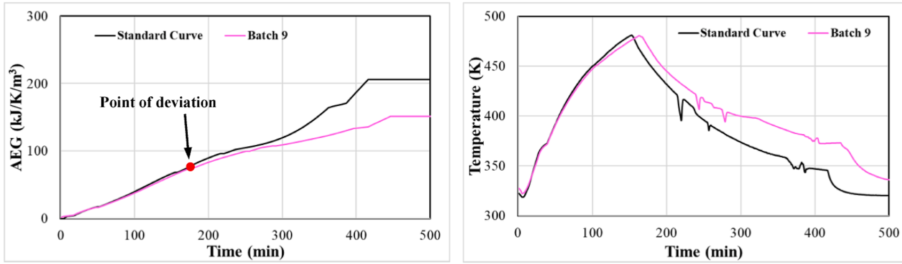

(a) (b)

Fig. 12. Comparison of Batch 9 with the standard batch (Batch 3) (a) Comparison of AEG value, (b) Comparison of grease temperature evolution.

editing, Validation, Investigation, Data curation. **Andrew Sanford:** Writing – review & editing, Investigation. **Jim Carroll:** Supervision. **M. M. Khonsari:** Writing – review & editing, Project administration, Funding acquisition, Conceptualization.

Declaration of competing interest

The authors declare that they have no known competing financial interests or personal relationships that could have appeared to influence the work reported in this paper.

Data availability

Data will be made available on request.

Acknowledgments

LSU authors greatly acknowledge the support of the LSU Board of Supervisors under Leveraging Innovation for Technology Transfer (LIFT[2]) Grant: LSU-2021-LIFT-013.

References

[1] ASTM standard D288-61. Definitions of terms relating to petroleum. 1978.
[2] Pintaude, G., Cousseau, T. and Rudawska, A. eds., 2022. *Tribology of Machine Elements: Fundamentals and Applications*. BoD–Books on Demand.
[3] X. Fan, X. Wei, Y. He, Z. Zhao, K. Lin, M. Zhu, MoS2 functionalized lithium complex soap with enhanced thickening net structure toward high-performance thickener, Chem. Eng. J. 478 (2023) 147445.
[4] C. Coe, Grease: a niche market opportunity, Tribology & Lubrication Technology 71 (5) (2015) 32.
[5] S.S. Rawat, A.P. Harsha, Current and future trends in grease lubrication, Automotive Tribology (2019) 147–182.
[6] P.A. Tanguy, F. Thibault, E. Brito-De La Fuente, T. Espinosa-Solares, A. Tecante, Mixing performance induced by coaxial flat blade-helical ribbon impellers rotating at different speeds, Chem. Eng. Sci. 52 (11) (1997) 1733–1741.
[7] L. Hamnelid, Introduction, in: C. Balan (Ed.), The Rheology of Lubricating Greases, European Lubricating Grease Institute, Amsterdam, 2000, p. 1.
[8] M.A. Delgado, M.C. Sánchez, C. Valencia, J.M. Franco, C. Gallegos, Relationship among microstructure, rheology and processing of a lithium lubricating grease, Chem. Eng. Res. Des. 83 (9) (2005) 1085–1092.
[9] A.E. Yousif, Rheological properties of lubricating greases, Wear 82 (1) (1982) 13–25.
[10] C. Balan, J.M. Franco, Influence of the geometry on the rotational rheometry of lubricating greases, The Rheology of Lubricating Greases (2000) 43–65.
[11] NLGI Lubricating Grease Production Survey. Available at www.nlgi.org/products-page/5-greaseproduction-survey.
[12] W.D. Weatherford Jr., M.L. Valtierra, P.M. Ku, Experimental study of spline wear and lubrication effects, Asle, Transactions 9 (2) (1966) 171–178.
[13] D. Scott, Further data on the effect of additives on the water induced pitting of ball bearings, J. Inst. Petrol 48 (457) (1962) 24.
[14] Loper, John T., and Jeremy P. Styer. Friction modifiers for lubricating oils. U.S. Patent 9,550,955, issued January 24, 2017.
[15] NLGI, Lubricating Grease Guide, National Lubricating Grease Institute, Kansas, 1994.
[16] Z. Li, Y. Li, S. Chen, Q. Zha, M. Zhu, In-situ monitoring of hydrogen peroxide production at nickel single-atom electrocatalyst, Chem. Eng. J. 460 (2023) 141657.
[17] J.M. Franco, M.A. Delgado, C. Valencia, M.C. Sánchez, C. Gallegos, Mixing rheometry for studying the manufacture of lubricating greases, Chemical Engineering Science 60 (8–9) (2005) 2409–2418.
[18] Huangqing Ye, Jian Xuchao, Ying Wang, Jun Long, Xiaofang Zhang, Junqin Wu, Yingying Pan, et al., Online and in-situ monitoring of the growth of silver nanowires and nanoparticles with conductive measurement, Chemical Engineering Journal 479 (2024) 147744.
[19] K.P. Lijesh, M.M. Khonsari, On the useful life of tribo-pairs experiencing variable loading and sliding speed, Wear 416 (2018) 103–114.
[20] M.A. Amooie, K.P. Lijesh, A. Mahmoudi, E. Azizian-Farsani, M.M. Khonsari, On the Characteristics of Fatigue Fracture with Rapid Frequency Change, Entropy 25 (6) (2023) 840.
[21] A. Rezasoltani, M.M. Khonsari, On the correlation between mechanical degradation of lubricating grease and entropy, Tribol. Lett. 56 (2014) 197–204.
[22] E. Kuhn, Analysis of a grease-lubricated contact from an energy point of view, Int. J. Mater. Prod. Technol. 38 (1) (2010) 5–15.
[23] Kuhn, Erik. "Friction and wear of a grease lubricated contact—An energetic approach." *Tribology-Fundamentals and Advancements* (2013).
[24] M.D. Bryant, M.M. Khonsari, F.F. Ling, On the thermodynamics of degradation, Proceedings of the Royal Society a: Mathematical, Physical and Engineering Sciences 464 (2096) (2008) 2001–2014.
[25] C. Jarzynski, Microscopic analysis of Clausius-Duhem processes, J. Stat. Phys. 96 (1) (1999) 415–427.
[26] J.A. Osara, Thermodynamics of manufacturing processes—the workpiece and the machinery, Inventions 4 (2) (2019) 28.
[27] J.A. Osara, M.D. Bryant, Thermodynamics of grease degradation, Tribol. Int. 137 (2019) 433–445.
[28] I. Prigogine, Etude thermodynamique des phenomenes irreversible, Bull. Acad. Roy. Blg. Cl. Sci. 31 (1945) 600–606.
[29] M. Naderi, M.M. Khonsari, Thermodynamic analysis of fatigue failure in a composite laminate, Mech. Mater. 46 (2012) 113–122.
[30] I. Prigogine, Introduction to thermodynamics of irreversible processes, 3rd edn, Interscience Publishers, Wiley, New York, NY, 1967.
[31] A. Bejan, Advanced engineering thermodynamics, Wiley, New York, NY, 1988.
[32] R. Müller, Laboratory methods for testing lubricants, Lubricants and Lubrication (2017) 881–902.
[33] K.P. Lijesh, M.M. Khonsari, Procedure for evaluating the mechanical degradation of a grease, NLGI Spokesman 84 (1) (2020) 24–35.
[34] M.AR. Mohammed, Effect of additives on the properties of different types of greases. Iraqi Journal of, Chem. Pet. Eng. 14 (3) (2013) 11–21.
[35] G. Gow, Lubricating grease, Chemistry and Technology of Lubricants (2010) 411–432.
[36] N. McGuire, Grease manufacturing: Chemistries and processes, Tribology & Lubrication Technology 73 (3) (2017) 32.
[37] Coleman, Richard L., Arnold C. Witte Jr, and Aubrey L. Stone. Process for manufacturing aluminum complex soap thickened grease. U.S. Patent 4,132,658, issued January 2, 1979.
[38] M. Naderi, M. Amiri, M.M. Khonsari, On the thermodynamic entropy of fatigue fracture, Proceedings of the Royal Society a: Mathematical, Physical and Engineering Sciences 466 (2114) (2010) 423–438.
[39] A. Mahmoudi, M.A. Amooie, K.P. Lijesh, M.M. Khonsari, In Situ Prediction of Metal Fatigue Life Using Frequency Change, Metals 13 (10) (2023) 1681.